Journal of Geriatric Cardiology (2015) 12: 394–401

Research Article · **Open Access** ·

Characterization of a Chinese KCNQ1 mutation (R259H) that shortens repolarization and causes short QT syndrome 2

Zhi-Juan WU[1*], Yun HUANG[2*], Yi-Cheng FU[1], Xiao-Jing ZHAO[1], Chao ZHU[1], Yu ZHANG[1], Bin XU[1], Qing-Lei ZHU[1], Yang LI[1]

[1]*Department of Cardiology, Chinese PLA General Hospital, 28 Fuxing Road, Beijing, China*
[2]*Department of Gerontology, Union Hospital, Tongji Medical College, Huazhong University of Science and Technology, Wuhan, China*

Abstract

Objectives To evaluate the association between a KCNQ1 mutation, R259H, and short QT syndrome (SQTS) and to explore the electrophysiological mechanisms underlying their association. **Methods** We performed genetic screening of SQTS genes in 25 probands and their family members (63 patients). We used direct sequencing to screen the exons and intron-exon boundaries of candidate genes that encode ion channels which contribute to the repolarization of the ventricular action potential, including KCNQ1, KCNH2, KCNE1, KCNE2, KCNJ2, CACNA1c, CACNB2b and CACNA2D1. In one of the 25 SQTS probands screened, we discovered a KCNQ1 mutation, R259H. We cloned R259H and transiently expressed it in HEK-293 cells; then, currents were recorded using whole cell patch clamp techniques. **Results** R259H-KCNQ1 showed significantly increased current density, which was approximately 3-fold larger than that of wild type (WT) after a depolarizing pulse at 1 s. The steady state voltage dependence of the activation and inactivation did not show significant differences between the WT and R259H mutation ($P > 0.05$), whereas the time constant of deactivation was markedly prolonged in the mutant compared with the WT in terms of the test potentials, which indicated that the deactivation of R259H was markedly slower than that of the WT. These results suggested that the R259H mutation can effectively increase the slowly activated delayed rectifier potassium current (I_{Ks}) in phase 3 of the cardiac action potential, which may be an infrequent cause of QT interval shortening. **Conclusions** R259H is a gain-of-function mutation of the KCNQ1 channel that is responsible for SQTS2. This is the first time that the R259H mutation was detected in Chinese people.

J Geriatr Cardiol 2015; 12: 394–401. doi:10.11909/j.issn.1671-5411.2015.04.002

Keywords: Ion channel; KCNQ1 gene; Mutation; Short QT syndrome; Slowly activated delayed rectifier potassium current

1 Introduction

Short QT Syndrome (SQTS) was originally defined in 2000 by markedly shortened QT intervals, poor rate adaptation of the QT interval, shortened ventricular and atrial refractory periods and atrial/ventricular arrhythmias, and it causes sudden cardiac death (SCD) in affected patients.[1] Although the risk of SCD has been reported to be high, the mechanisms underlying the disease are not well understood because of the small number of cases identified.[2] Candidate gene screening has revealed that the variants of the potassium channel coding gene, KCNQ1 (also called KvLQT1 or Kv7.1), were closely associated with SQTS2.[3] Chen, *et al*.[4] first reported the S140G gain-of-function mutation in KCNQ1 in familial atrial fibrillation without a QT abnormality. Then, additional gain-of-function mutations, including the V141M, S209P, V307L and Q147R mutations, were gradually proposed, of which the V141M and V307L mutations were considered to be highly associated with SQTS.[5–7] Recently, the R259H variant was identified in SQTS patients by Mazzanti, *et al*.[8] Here, we present data of 63 Chinese SQTS patients and characterize the R259H variant.

2 Methods

2.1 Subjects and sample collection

Electrocardiogram (ECG), echocardiogram, Holter recording and exercise stress testing were performed in the probands of SQTS and their family members. We studied 63 patients (25 probands and 38 family members) with a QTc interval ≤ 350 ms with or without a history of cardiac

*The first two authors contributed equally to this manuscript.
Correspondence to: Yang LI, MD, Department of Cardiology, Chinese PLA General Hospital, 28 Fuxing Road, Beijing, China.
E-mail: liyangbsh@163.com
Telephone: +86-10-66936762 **Fax:** +86-10-66936762
Received: December 22, 2014 **Revised:** March 24, 2015
Accepted: April 27, 2015 **Published online:** May 20, 2015

arrest, or SCD. We performed genetic screening of SQTS genes in 25 families (63 patients). The blood samples were collected from all probands and their family members for genome-wide DNA analysis. Written informed consent was obtained from each participant. The study protocol was approved by the Chinese PLA General Hospital Ethical Committee.

2.2 Genetic analysis

We used direct sequencing to screen the exons and intron-exon boundaries of candidate genes that encode ion channels that contribute to the repolarization of the ventricular action potential, including KCNQ1, KCNH2, KCNE1, KCNE2, KCNJ2, CACNA1c, CACNB2b and CACNA2D1. All of the gene mutations were identified using standard genetic tests, as previously reported.[9] Mutation screening was performed on genomic DNA that was extracted from peripheral blood lymphocytes using standard techniques. The entire KCNQ1 coding region was analyzed using PCR-DNA sequencing to screen the mutations. DNA sequence variation was validated by sequencing two independent PCR products and secondarily by primer-induced restriction enzyme digestion.

2.3 Transfection in HEK-293 cells

Wild type (WT) and the R259H mutation of KCNQ1 cDNAs were cloned in the eukaryotic expression vector pcDNA3.1. The analysis of KCNQ1 expression and localization was conducted in human embryonic kidney (HEK) 293 cells after transient transfection (48–72 h). The HEK-293 cells were cultured in minimal essential medium (MEM; Gibco BRL, USA) containing 10% heat inactivated fetal bovine serum (FBS; Gibco BRL, USA), 100 μg/mL penicillin and 100 μg/mL streptomycin (complete media) at 37°C in a humidified atmosphere containing 5% CO_2. The α (KCNQ1) subunit and β (KCNE1) subunit co-assembled into the slowly activating delayed rectifier potassium channel (I_{Ks}). Transient transfection of the KCNQ1 channel cDNA (WT or R259H plasmid pcDNA3.1, 0.6 μg) and KCNE1 (pcDNA3.1, 0.6 μg) into the cultured cells was performed using Lipofectamine 2000 (Life Technologies, USA) following the manufacturer's instructions. CD8 cDNA was co-transfected to be used as a reporter gene (EBo-pCD vector, American Type Culture Collection, USA). CD8-positive cells were identified using Dynabeads (Dynal, M-450 CD8), and the cells were harvested 48–72 h after transfection.

2.4 Patch clamp experiments

The HEK-293 cells were bathed in a solution containing (in mmol/L) NaCl 140, KCl 4, $CaCl_2$ 2, $MgCl_2$ 1, HEPES 10 and glucose 5, adjusted to pH 7.4 with NaOH. Current was recorded using a whole cell patch-clamp technique with a MultiClamp 700B amplifier (Axon Instruments, USA). All signals were acquired at 5 kHz (Digidata 1322A, Axon Instruments, USA). Patch pipettes were pulled from borosilicate glass on a P-97 horizontal puller (Sutter Instruments, USA). The electrodes had a resistance of 2–3 MΩ.

For recording the K^+ currents, pipettes were filled with the following (in mmol/L): KAsp 140, EGTA 10, MgATP 4, $MgCl_2$ 1, HEPES 10, adjusted to pH 7.3 with KOH. The HEK-293 cells were superfused with solution containing the following (in mmol/L): NaCl 140, $CaCl_2$ 1, $MgCl_2$ 1, KCl 4, HEPES 10, and glucose 5, adjusted to pH 7.4 with NaOH. To ensure reproducibility, after the whole-cell conditions were established by rupturing the cell membrane, we allowed a dialysis period of 4 min before beginning the measurements of any of the control records. During the dialysis period, we monitored the current-voltage relationships to ensure stability and consistency in the recordings. The holding potential was −80 mV, and the inter-pulse interval was at least 15 s. A routine series resistance compensation was performed for values > 80% to minimize voltage clamp errors. The membrane capacitance was measured on each of the cells, and it was compensated by approximately 80%–90% of their initial value. Currents were elicited every 25 s by stepping the membrane to a test potential between −120 mV and +80 mV in 10 mV increments. Current densities were calculated as current (pA) divided by cell capacitance (pF). Tail current was recorded at –40 mV and −120 mV for 3 s each. Voltage activation data were plotted as the peak and tail current amplitudes and were normalized to the maximal value against the test potential values and fitted to a Boltzmann distribution. The activation curves were derived from the current values during a repolarization step to −120 mV after a series of 1.5 s depolarizations. Steady-state activation and inactivation of the current was induced by voltage steps between −80 mV and +60 mV for 2 s, following a test pulse of +60 mV for 2 s from a holding potential of –120 mV. The deactivation of current was induced by a condition pulse of +60 mV for 3 s from a holding potential of –80 mV, following test pulses from −140 mV to –20 mV for 5 s with 20 mV steps. The time course of the deactivation was fitted by a single exponential function.

2.5 Western blotting

The HEK-293 cells were lysed in RIPA lysis buffer supplemented with 1 mmol/L phenylmethyl sulfonyl fluoride (PMSF, Amresco, USA) after transient transfection (48 h). Proteins were boiled at 100°C for 5 min in loading buffer. After the proteins were transferred to polyvinylidene di-

fluoride membranes, the membranes were blocked with 5% milk and incubated overnight with a primary antibody against KCNQ1 at a density of 5 μg/mL (Abcam, USA). The secondary antibody was rabbit anti-mouse IgG (Abcam, USA) at 1: 3,000 for 60 min at room temperature. Detection was performed using the ECL Plus kit following the manufacturer's instructions (Amersham Pharmacia).

2.6 Data analysis

Off-line leak correction was performed on all amplitude data. Data were presented as mean ± SE, with N representing the number of cells analyzed. The pCLAMP version 9.2 (Axon Instruments, USA) and Origin (Microcal Software) software were used for the data analysis. $P < 0.05$ was considered statistically significant according to Student's *t*-test analysis.

3 Results

3.1 Clinical features and mutation analysis

In our study, the third SQTS2 gene mutation, R259H, was implicated in the shortening of the QT interval. Of the 25 probands and 38 family members who were referred to our center with a QTc interval ≤ 350ms and a history of cardiac arrest or SCD, a 20-year-old proband (Ⅲ-1) was found to be genopositive, who exhibited aborted cardiac arrest at rest. The ECG of this proband showed a shortened QT/QTc interval of 290/310 ms (Figure 1 A). Later, an ICD was implanted, and after two years, another episode of ventricular fibrillation was successfully treated by the device. His family was further investigated, and two generations and eight family members (five males and four females) were included in the genetic analysis (Figure 1 B). The proband's mother (II-2), who was 46 years old at the time of presentation, also showed a shortened QT/QTc interval of 285/300 ms on the resting ECG and complained of previous episodes of paroxysmal ventricular tachycardia (PVT). The proband's cousin (Ⅲ-2) suffered sudden unexpected death at the age of 28 years. Other family members presented with normal ECG and QTc duration. Further blood genetic screening identified a heterozygous KCNQ1 missense mutation with a nucleotide substitution of cytosine to thymine at position 259 (c.259C > T) that leads to

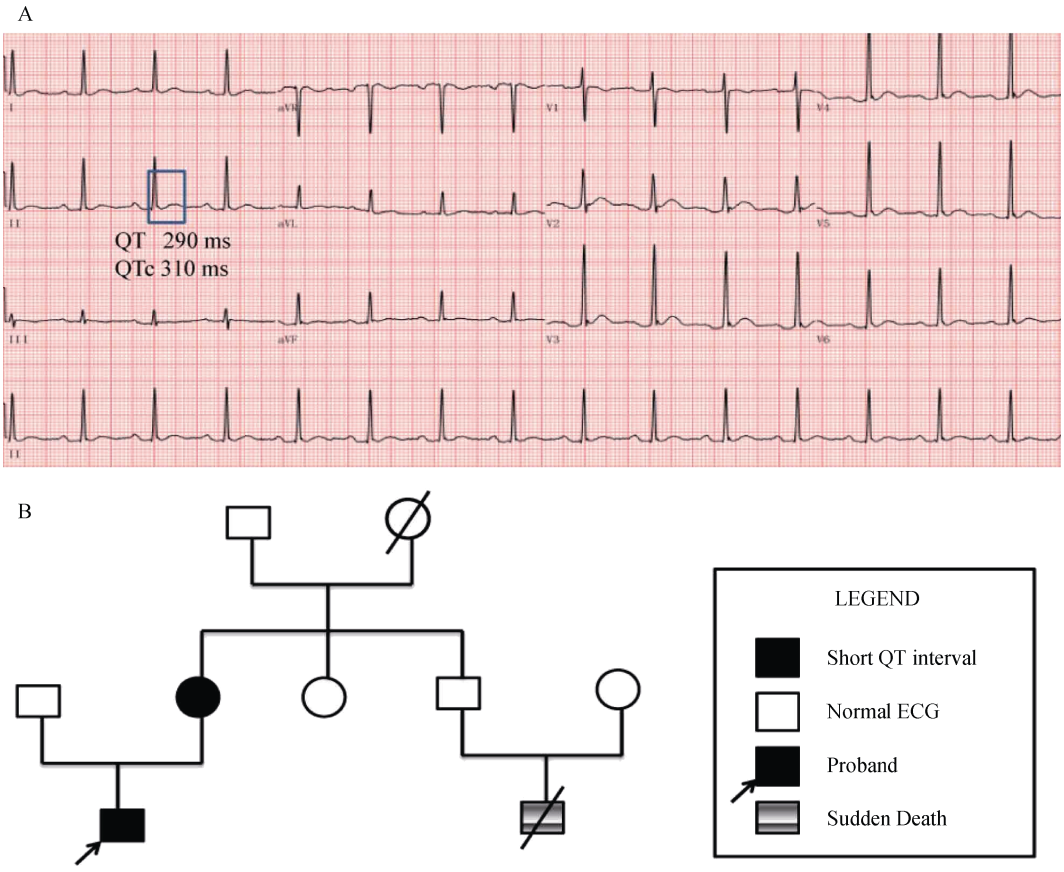

Figure 1. Pedigree of the short QT syndrome family. (A): ECG of the proband; (B): family investigation. The proband (denoted by the arrow); circles indicate female family members; squares indicate male family members; solid symbols indicate a person with a short QT interval; symbols with a slash indicate deceased family members. ECG: electrocardiogram; QTc: corrected QT.

an amino acid change from arginine to histidine (R259H). This applies equally to his mother (II-2) based on DNA sequencing. The mutation was located in the KCNQ1 gene regions and was confirmed upon restriction analysis (data not shown). The phenotype based on the R259H gain-of-function mutation in the KCNQ1 subunit may allow for the alteration of channel gating and altered functional KCNE modulation based on heterologous expression experiments.

3.2 Characterization of the R259H mutation on channel function

To determine the mechanism by which the R259H mutation modulates KCNQ1, reduces action potential duration, and shortens the QT interval, we co-expressed R259H-KCNQ1 with the KCNE1 channel. The functional consequences of the R259H mutation and WT were characterized using conventional whole cell voltage clamp protocols. Here, we report the results of detailed investigations of this mutant, which indicates a novel electrophysiological mechanism for gain-of-function KCNQ1 mutations.

3.2.1 Changes in the current and I-V relationship curve of WT-KCNQ1 and R259H-KCNQ1

With a holding potential of –40 mV, channel activation was obtained using a step protocol from –120 mV to +80 mV for 4 s. As shown in Figure 2A&C, the R259H current shape was a typical rectangle; Figure 2A&C also represent the tail currents recorded under –40 mV and –12 mV conditions, respectively. The R259H-KCNQ1 peak current density was significantly increased WT: 173.2 ± 28.5 *vs*. 86.9 ± 16.9 pA/pF (n = 13, P < 0.05), respectively, as shown in Figure 2 B and E. The R259H tail current at the holding potential of –40 mV was significantly larger than that of WT (R259H WT: 65.3 ± 8.6 pA/pF *vs*. 29.7 ± 8.5 pA/pF, respectively, n = 13, P < 0.05) as shown in Figure 2 D and E. Interestingly, the test potentials less than 0 mV elicited relatively little WT and R259H, but when the test potentials exceeded 0 mV, a markedly larger R259H-KCNQ1 was observed as shown in Figure 2D, which was quite different from those of the V307L or V141M mutants. No significant differences in the tail current densities were highlighted when the holding potential was –120 mV (R259H: –21.7 ± 5.7 pA/pF *vs*. WT: –24.2 ± 4.7 pA/pF, n = 13, P > 0.05) as shown in Figure 2E and F.

3.2.2 Peak current of different depolarization time with WT-KCNQ1 and R259H-KCNQ1

I_{Ks} was elicited in simulated voltage-clamp experiments with voltage from –120 mV to +80 mV for 4 s. The mean currents measured 1 or 4 s after the step changes in the membrane voltage are compared in Figure 3 for both R259H-KCNQ1 and WT-KCNQ1. As shown in Figure 3A–C, the R259H current density was approximately 3-fold larger than WT after a 1 s depolarizing pulse, whereas the difference with WT was less marked at 4 s, which

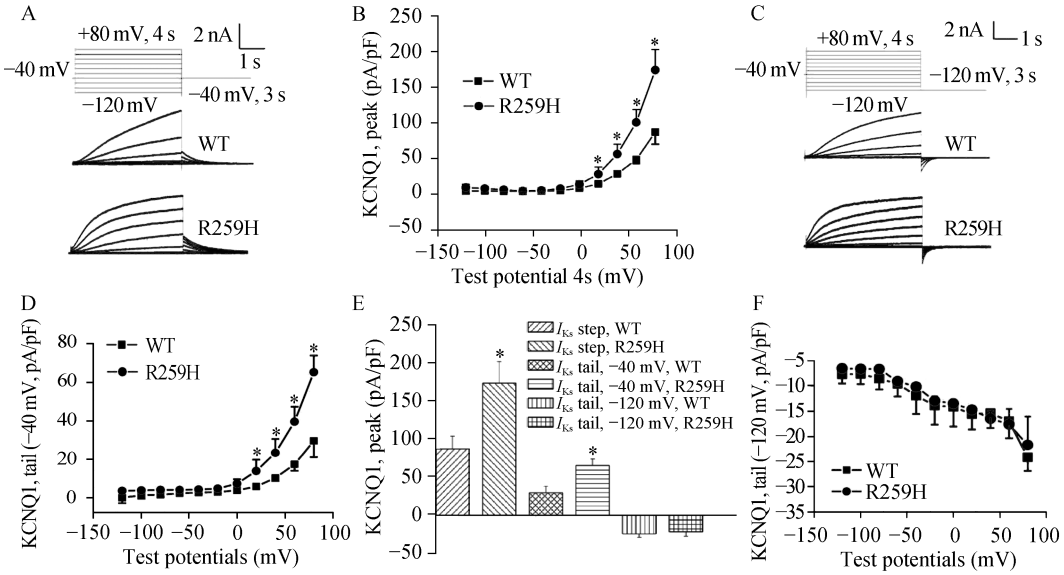

Figure 2. The current densities of WT-KCNQ1 and R259H-KCNQ1. (A): Schematic representation of the voltage-clamp protocol and the representative WT and R259H current traces; (B): The peak I-V relationships for I_{Ks} under WT and R259H conditions; (C): Tail current was recorded at –120 mV for 3000 ms; (D): The tail I-V relationships for I_{Ks} under WT and R259H conditions at a voltage of –40 mV; (E): The comparison of the current density of the peak and step between the WT and R259H condition under different conditions; (F): The tail I-V relations for I_{Ks} under WT and R259H conditions at a voltage of –120 mV. *P < 0.05. WT: wild type.

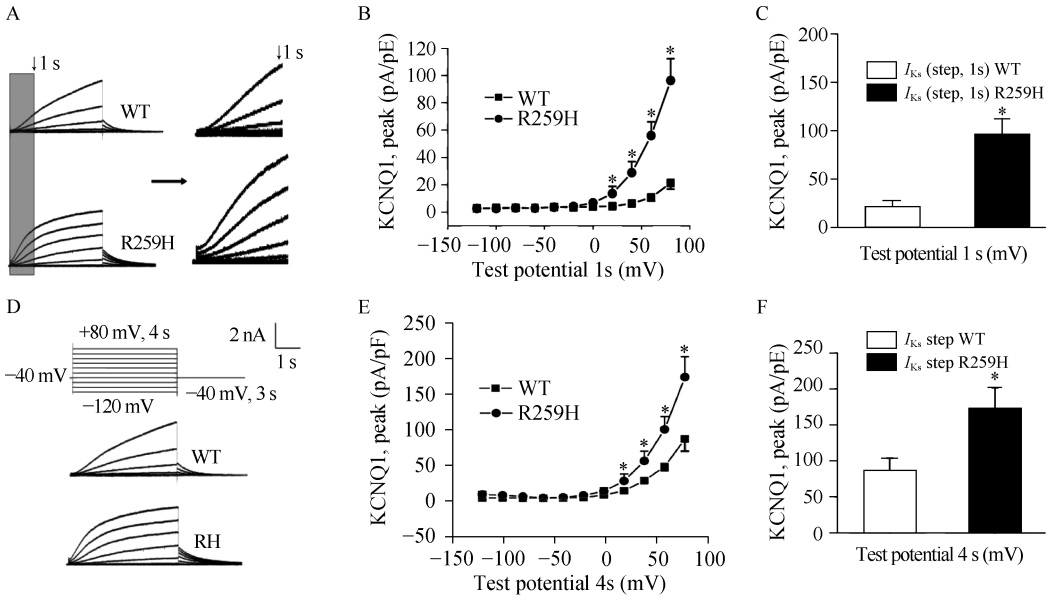

Figure 3. The comparison of the current between the WT and R259H condition under the simulated time of 4 s and 1 s. (A): I_{Ks} was elicited in simulated voltage-clamp experiments measured 1 s into the imposed voltage commands; (B): The peak I–V relationships for I_{Ks} under WT and R259H conditions at the simulated time of 1 s; (C): The density of the R259H current was approximately 3-fold larger than WT after a 1 s depolarizing pulse; (D): I_{Ks} was elicited in simulated voltage-clamp experiments measured 4 s into the imposed voltage commands; (E): The peak I–V relationships for I_{Ks} under WT and R259H conditions at the simulated time of 4 s; and (F): The density of the R259H current was approximately 2-fold larger than WT after a 4 s depolarizing pulse. *P < 0.05. WT: wild type.

suggested that the kinetics of activation in the mutant was faster than that of the WT (activation time constant R259H: 349.9 ± 16.9 ms WT: 630.1 ± 27.7 ms, P < 0.05). The differences were less marked at 4 s of the depolarizing pulse, as shown in Figure 3D–F. This indicates that the kinetics of activation in the mutant was faster than that of the WT, suggesting that the R259H mutation was a gain of function mutation in the KCNQ1 channel and might shorten the action potential duration and lead to a decrease in the QT interval.

3.2.3 Gating kinetics of the WT-KCNQ1 and R259H-KCNQ1

Steady-state activation (SSA) and steady-state inactivation (SSI) curves were fitted using a Boltzmann distribution as follows: $G_{(t)}/G_{max} = 1/[1 + \exp(V_m - V_{1/2})]$, where $V_{1/2}$ is the half-maximal activation/inactivation voltage, Vm is the test membrane potential, and k is the slope factor. As shown in Figure 4 A to F, we observed that the SSA and SSI did not exhibit significant differences between the WT and the R259H mutation (SSA: $V_{1/2,\ WT}$ = 15.4 ± 3.3 mV, k_{WT} = 19.4 ± 4.2, $V_{1/2,\ R259H}$ = 13.4 ± 2.0 mV, k_{R259H} = 18.0 ± 2.2; SSI: $V_{1/2,\ WT}$ = −12.1 ± 1.5 mV, k_{WT} = 14.3 ± 1.8, $V_{1/2,\ R259H}$ = −9.0 ± 3.9 mV, k_{R259H} = 13.1 ± 2.4; n = 13, P > 0.05). The kinetics of deactivation were studied based on test potential pulses from −140 mV to −20 mV, whereas the time constants of deactivation were determined by fitting the current recordings with a double exponential function. In contrast, the deactivation of R259H was markedly slower than WT-KCNQ1 deactivation, and the results were shown both in the current records in Figure 4G and the time constant plots shown in Figure 4H. The time constant of deactivation was slower for R259H than for WT-KCNQ1 across all plotted voltages (from −120 mV to −20 mV). R259H produced a prolongation of the time constant of deactivation (> −80 mV), which suggested a slower deactivation procedure, with a Tau value of 3,113.0 ± 175.0 ms in the R259H-KCNQ1 and 1778.4 ± 193.4 ms in the WT channel (n = 14, P < 0.05, shown in Figure 4I); this prolongation could partly explain the higher current recorded in the R259H mutant.

3.2.4 Analysis of the cellular distribution

Western blot anti-KCNQ1 was conducted after transient transfection in HEK-293 cells for 48 h. The expression levels of the WT and R295H mutants in the HEK-293 cells are similar, as shown in Figure 5. This phenomenon indicates that the higher current recorded in the R259H mutant is the result of a faster activation and a slower deactivation and not of the change in the quantity of the channel protein.

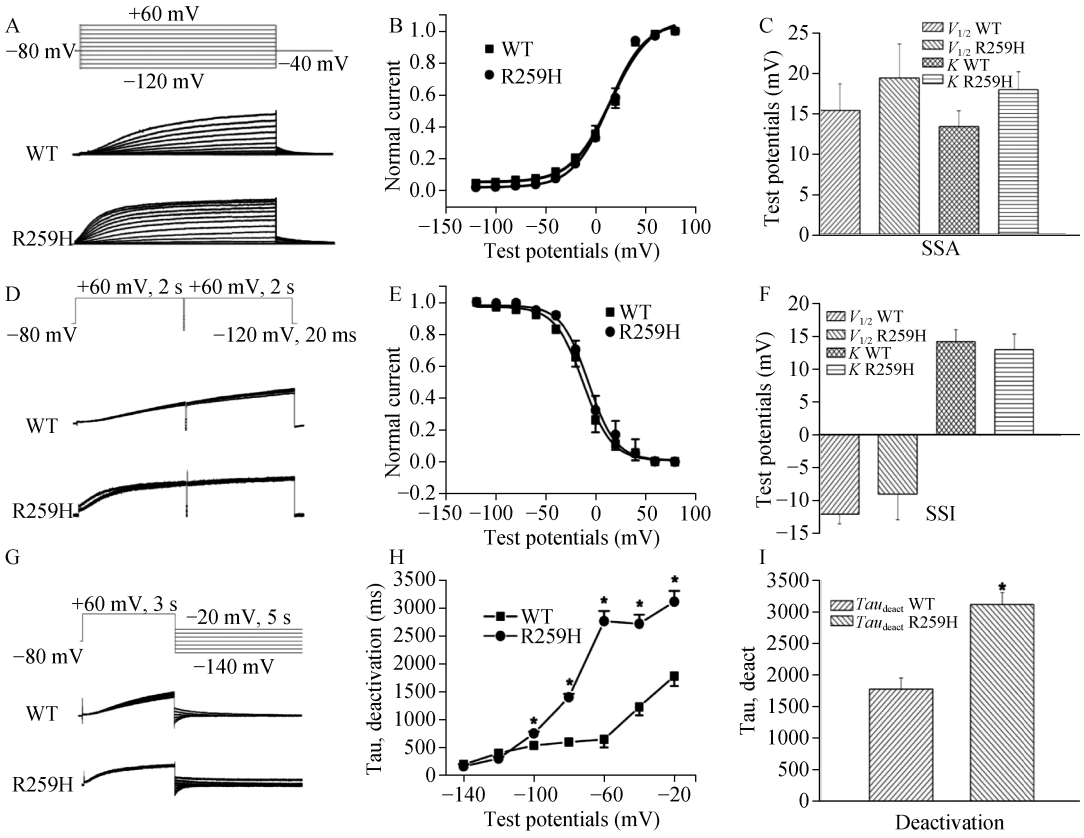

Figure 4. The steady-state activation, inactivation and deactivation of KCNQ1/KCNE1. (A): I_{Ks} was activated under WT-KCNQ1 and R259H-KCNQ1 conditions; (B): SSA curves are shown under WT-KCNQ1 and R259H-KCNQ1 conditions; (C): time constants of SSA under WT-KCNQ1 and R259H-KCNQ1 conditions; (D): representative inactivation current traces recorded from WT and R259H; (E): SSI curves are shown under WT-KCNQ1 and R259H-KCNQ1 conditions; (F): time constants of SSI under WT-KCNQ1 and R259H-KCNQ1 conditions; (G): representative deactivation current traces recorded from WT and R259H; (H): time constants of deactivation under WT-KCNQ1 and R259H-KCNQ1 conditions; and (I): comparison of Tau value under WT-KCNQ1 and R259H-KCNQ1 conditions. *P < 0.05. SSA: steady-state activation; SSI: steady-state inactivation; WT: wild type.

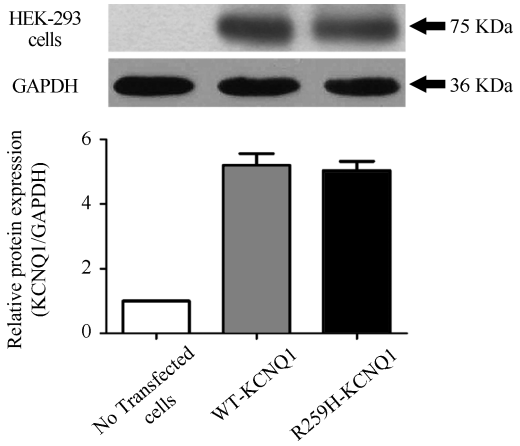

Figure 5. Analysis of the cellular distribution. Western blot with anti-KCNQ1 (Kv7.1) after transient transfection in HEK-293 cells. The expression levels of the R295H mutant are similar as that of WT. GAPDH: glyceraldehyde-3-phosphate dehydrogenase; WT: wild type.

4 Discussion

SQTS is a rare autosomal dominant, congenital electrical disorder with low penetrance and is associated with typically abnormal short QT-intervals and a propensity to develop potentially lethal ventricular arrhythmias.[3] It is important to supplement the paucity of data on SQTS in terms of its genotype-phenotype correlation, which may be useful for guiding risk-stratification, diagnosis and treatment of the disease. We have investigated the mechanism underlying the significant increase in I_{Ks} by the KCNQ1 R259H SQTS2 mutant. We found that the R259H mutant interacts with the WT-KCNQ1 subunits and that this interaction causes a gain-of-function of the I_{Ks} current. This is the first study to report a novel SQTS2 mutant (R259H) identified in one of 25 SQTS probands that were screened, which is the third mutation on this gene reported worldwide. This is also the

first study to show the detailed electrophysiological characterization of this novel mutation.

4.1 Function of the R259H mutant in the KCNQ1 channel

The familial nature and arrhythmic potential of SQTS2 was reported only in a single sporadic patient.[10] The R259H mutation was identified in a sporadic severe SQTS case presenting with documented ventricular fibrillation and appropriate ICD interventions; the resting electrocardiogram observed a QT/QTc interval of 290/310 ms in this case. Then, additional experiments have been conducted to thoroughly investigate the mechanisms underlying how this mutation affects the kinetics of KCNQ1. In our research, we found two important electrophysiological characteristics of the R259H mutant. First, our results showed that the current shape of the R259H-KCNQ1 changed into a typical rectangle compared with the WT-KCNQ1. The patch-clamp data revealed that the peak current density of R259H-KCNQ1 was approximately 3-fold higher with a 1 s depolarizing pulse compared with that of WT-KCNQ1, and the differences were less marked at 4 s, suggesting that the activation kinetics of R259H-KCNQ1 was faster than that of the WT. Second, we found that the R259H mutant shifted the deactivation of KCNQ1 towards more positive potentials, but the steady state voltage dependence of activation and inactivation did not show significant differences between the WT and the R259H mutation. All of these findings indicate that R259H caused a significant increase in I_{Ks} current density, which not only slowed the I_{Ks} current deactivation but also accelerated the activation kinetics, thus providing a gain of function mechanism. The functional increase in R259H-I_{Ks} may affect the action potential duration of cardiac myocytes, leading to the shortening of the QT interval, which in turn causes cardiac arrhythmias.

4.2 The mechanism of the increased R259H-KCNQ1 current density

In the present study, the R259H mutant showed an increased step and tail current density by approximately 2-fold of that of the WT, and the peak current density was approximately 3-fold higher than that of the WT after a 1 s depolarizing pulse, whereas with a 4 s depolarizing pulse, the differences were less marked. Thus, clearly accelerated activation as well as a positive shift in the channel availability contributes to the increase in the current density, resulting in significant augmentation of the current amplitude induced by the fast activation due to a positive shift in voltage dependent activation. Unlike the other two previously reported mutants, R259H increased quickly after beginning and increased slowly with further stimulation changing the shape of the current into a rectangle. According to previous reports by Bellocq and Hong, V307L-KCNQ1 and V141M-KCNQ1 are both rapidly activating voltage-dependent K^+ selective currents; however, their effects on the peak and tail current densities are limited, so the current amplitudes for the WT and mutant channels are similar.[6,12] This feature of R259H might partly indicate that the mutant channels were activated faster and recruited earlier during the cardiac action potential, thus providing gain of function mechanisms.

4.3 The Consequence of slowed deactivation of R259H-KCNQ1

In our experiments, we used cloned R259H-KCNQ1 channels expressed in HEK-293 cells to analyze the electrophysiological properties between the R259H mutant channel and WT. We found that the main reasons for the increased R259H-KCNQ1 were its prolonged deactivation time constant and its slowed deactivation procedure. The data revealed that the time constant of recovery from the deactivated R259H mutation channel was much slower than that of WT, ranging from −80 mV to +60 mV. The negative shift in the R259H-KCNQ1 channel deactivation results in higher numbers of channels available to constitutively open within phase 3 of the action potential, which leads to dysfunction of the cardiac repolarization and excessive APD shortening.[12]

Our data indicated that there are some connections in the gating properties between R259H and V307L. Although the two SQTS2 mutants have similar gain-of-function effects on KCNQ1 channels, their electrophysiological mechanisms are quite different. The V307L mutant induces a pronounced shift in the half-activation potential and an acceleration of the activation kinetics of KCNQ1, and its deactivating currents at various test-pulse potentials after depolarization to 60 mV were not significantly different compared to WT.[13] In contrast, the major influence of R259H lies in its deactivation course of KCNQ1, not in its steady-state activation or inactivation kinetics.

4.4 Clinical perspective and study limitation

Obviously, the best way to restore the action potential duration toward control levels in SQTS2 patients is to promote Kv7.1 channel function.[2] However, due to the limited number of cases, the characteristics and effective treatment methods for SQTS are not well understood. Very little information has been provided about whether the mutant affected gain-of-function I_{Ks} channels act not only through a net increase in the current but also through other additional

mechanisms such as channel subunit-subunit interactions, membrane expression of mutant channels or intercellular ionic communications.[13] In this study, although our data suggested that the KCNQ1 mutations are most likely an infrequent cause of SQTS (< 10%), we could not perform extensive genetic testing or molecular biology methods to exclude the possibility of the presence of other affected factors. In addition, it is likely that similar types of KCNQ1 mutations with the function of current enhancement may work quite differently on one specific pathogenic mechanism. For example, Lundby, *et al*.[14] reported that one of the KCNQ1 gene variants, Q147R, leads to the heterogeneous distribution of Kv7.1 accessory subunits in the heart, which in turn leads to a Kv7.1 gain of function in the atria in familial atrial fibrillation but a Kv7.1 loss of function in the ventricles in QT prolongation. Based on these considerations, further efforts will be needed to investigate additional underlying mechanisms of R259H gene expression processes and the membrane distribution of R259H-KNCQ1 channels, using knock-in mice, induced pluripotent stem cells and computational SQTS models.

4.5 Conclusions

The R259H-KCNQ1 demonstrates a markedly increased current density and slowed deactivation, alters the channel electrophysiological properties and causes gain of function I_{Ks}, which may help to explain the enhancement of I_{Ks} in SQTS2. We determined a novel molecular mechanism and fully tested the hypothesis that the gain-of-function R259H mutation affects the I_{Ks} and results in the shortening of the QT interval, which provides a substrate for re-entrant arrhythmias.

Acknowledgment

This work was supported by grants obtained from the National Natural Science Foundation of China (No.: 81170177, 81030002) and science and Technology Department of Gansu Province Project (145RJZ104). The funders had no role in the study design, data collection and analysis, decision to publish, or preparation of the manuscript. Moreover, we are grateful for all the patients who have participated in this study. The authors declared no conflict of interest.

References

1 Gussak I, Brugada P, Brugada J, *et al*. Idiopathic short QT interval: a new clinical syndrome? *Cardiology* 2000; 94: 99–102.
2 Christian T, Jelena-Rima G, Jean-Se´bastien R, *et al*. Identification of a novel loss-of-function calcium channel gene mutation in short QT syndrome (SQTS6). *Eur Heart J* 2011; 32: 1077–1088.
3 Brugada J, Gussak I, Brugada P. Short QT syndrome: a predictable story. *Cardiology* 2014; 128: 231–233.
4 Chen YH, Xu SJ, Bendahhou S, *et al*. KCNQ1 gain-of-function mutation in familial atrial fibrillation. *Science* 2003; 299: 251–254.
5 Restier L, Cheng L, Sanguinetti MC. Mechanisms by which atrial fibrillation-associated mutations in the S1 domain of KCNQ1 slow deactivation of I_{Ks} channels. *J Physiol* 2008; 586: 4179–4191.
6 Hong K, Piper DR, Diaz-Valdecantos A, *et al*. De novo KCNQ1 mutation responsible for atrial fibrillation and short QT syndrome in utero. *Cardiovasc Res* 2005; 68: 433–440.
7 Das S, Makino S, Melman YF, *et al*. Mutation in the S3 segment of KCNQ1 results in familial lone atrial fibrillation. *Heart Rhythm* 2009; 6: 1146–1153.
8 Mazzanti A, Kanthan A, Monteforte N, *et al*. Novel insight into the natural history of short QT syndrome. *J Am Coll Cardiol* 2014; 63: 1300–1308.
9 Qureshi SF, Ali A, Ananthapur V, *et al*. Novel mutations of KCNQ1 in long QT syndrome. *Indian Heart J* 2013; 65: 552–560.
10 Crotti L, Taravelli E, Girardengo G, *et al*. Congenital short QT syndrome. *Indian Pacing Electrophysiol J* 2010; 10: 86–95.
11 Patel C, Yan GX, Antzelevitch C. Short QT syndrome: from bench to bedside. *Circ Arrhythm Electrophysiol* 2010; 3: 401–408.
12 Bellocq C, van Ginneken AC, Bezzina CR, *et al*. Mutation in the KCNQ1 gene leading to the short QT-interval syndrome. *Circulation* 2004; 109: 2394–2397.
13 Abriel H, Zaklyazminskaya EV. Cardiac channelopathies: Genetic and molecular mechanisms. *Gene* 2013; 517: 1–11.
14 Lundby A, Ravn LS, Svendsen JH, *et al*. KCNQ1 mutation Q147R is associated with atrial fibrillation and prolonged QT interval. *Heart Rhythm* 2007; 4: 1532–1541.